

Phase diagram of neutron-rich nuclear matter and its impact on astrophysics

F Gulminelli¹, Ad R Raduta², J Margueron³, P Papakonstantinou³
and M Oertel⁴

¹ CNRS, ENSICAEN, UMR6534, LPC ,F-14050 Caen cédex, France

² NIPNE, Bucharest-Magurele, POB-MG6, Romania

³ IPNO, CNRS/IN2P3, Université Paris - Sud 11, F-91406 Orsay cedex, France

⁴ LUTH, CNRS, Observatoire de Paris, Université Paris Diderot, 5 place Jules Janssen, 92195 Meudon, France

E-mail: gulminelli@lpccaen.in2p3.fr

Abstract. Dense matter as it can be found in core-collapse supernovae and neutron stars is expected to exhibit different phase transitions which impact the matter composition and equation of state, with important consequences on the dynamics of core-collapse supernova explosion and on the structure of neutron stars. In this paper we will address the specific phenomenology of two of such transitions, namely the crust-core solid-liquid transition at sub-saturation density, and the possible strange transition at super-saturation density in the presence of hyperonic degrees of freedom. Concerning the neutron star crust-core phase transition at zero and finite temperature, it will be shown that, as a consequence of the presence of long-range Coulomb interactions, the equivalence of statistical ensembles is violated and a clusterized phase is expected which is not accessible in the grand-canonical ensemble. A specific quasi-particle model will be introduced to illustrate this anomalous thermodynamics and some quantitative results relevant for the supernova dynamics will be shown. The opening of hyperonic degrees of freedom at higher densities corresponding to the neutron stars core modifies the equation of state. The general characteristics and order of phase transitions in this regime will be analyzed in the framework of a self-consistent mean-field approach.

1. Introduction

Triggered by the first data taking of X and gamma satellites, as well as by the improved capabilities of radio telescopes and high and ultra-high gamma ray detectors, there has been in the last ten years an impressive accumulation of observational data on supernova and neutron stars in different environments and at different evolution stages. Among the most important recent results one should mention the precise measurement of a very massive two solar-mass neutron star [1] which challenges a number of theoretical equations of state of dense matter, and the measurement of the cooling curve of the young pulsar Cassiopeia A [2], which gives strong constraints on the super-fluid properties of neutron star cores.

Understanding these data requires a good modelization of the supernova dynamics and of the formation process of neutron stars [3, 4], but also a precise and detailed control of the relevant microphysics. Sophisticated two and three-dimensional core-collapse supernova simulations show that matter in the supernova core explores a very large interval of baryonic densities, ranging from about $\rho > 10^{10} \text{ g} \cdot \text{cm}^{-3} \approx 10^{-4} \rho_0$ to several times the normal nuclear density ρ_0 ,

temperatures between some hundreds of keV and around 80 MeV, and proton fractions between ≈ 0.5 and ≈ 0.1 .

Different microscopic properties of nuclear matter in these wide thermodynamic conditions are of influence for these astrophysical phenomena. In particular, the core-collapse gravitational models show an important influence of the explosion mechanism with respect to the equation of state. To give an example, the explosion of very massive 15 solar-mass progenitors can presently only be achieved with a so-called "soft" equation of state.

In the whole sub-saturation region matter is not uniform but it is constituted of finite nuclei, with a dominance of exotic neutron-rich isotopes. Therefore a reliable calculation of the abundances of these nuclei is essential, as well as a knowledge of their mass, level densities and in-medium self-energy modifications.

Another key aspect concerns the thermal energy evacuation during the explosion and the proto-neutron star cooling. In the first evolution stage, heat is evacuated essentially by electron capture processes followed by neutrino emission. It is therefore very important to control the associated electro-weak processes, namely the electron capture rates and the neutrino interactions with the dense matter and the different nuclei of the proto-neutron star crust.

Both the equation of state and the neutrino cross sections are strongly influenced by the possible presence of phase transitions in dense matter. In particular, first-order phase transitions lead to a softening of the baryonic pressure, while second order phase transitions lead to a dramatic increase of the electroweak interaction probability [5]. For this reason, a control of the phase diagram of stellar matter is of importance in our understanding of these complex astrophysical process.

In this contribution, we will limit ourselves to the thermodynamic conditions where matter can be described by nucleonic or hadronic degrees of freedom and will examine two phase transitions which are expected to play a role in supernova physics, namely the crust-core phase transition at sub-saturation density and the possible phase transition towards strange matter at super-saturation density.

2. Sub-saturation densities and the quenching of the first-order phase transition

Since the early days of the equation of state modelization it was clearly recognized that, because of the strong similarities between the effective nucleon-nucleon potential and molecular interactions, the phase diagram of diluted nuclear matter should present a first-order phase transition of the liquid-gas type, terminating at high temperature and density in a critical point [6]. This conjecture has been confirmed in all phenomenological [7, 8] or microscopic [9] modelizations of symmetric and asymmetric nuclear matter with realistic effective interactions compatible with recent nuclear data.

In these calculations, nuclear matter is defined as an idealized bulk medium of neutrons and protons where the electromagnetic interaction is artificially switched off in order to achieve a thermodynamic limit. In the physical situation of stellar matter, however, charge neutrality is achieved by the screening effect of electrons on the proton charge. Because of the very different mass between electrons and protons, the compressibility of electron and proton matter is very different, which induces Coulomb effects that drastically modify the liquid-gas phase transition associated to uncharged nuclear matter. Specifically, in all density and temperature conditions relevant for neutron star physics, the electron charge can be safely considered as uniformly distributed [11]. This means that any baryonic density fluctuation (which is correlated to a proton density fluctuation because of the repulsive symmetry energy) induces a fluctuation in the electric charge. A well known consequence of the resulting Coulomb correlations is that the low density phase at zero temperature is not a gas, but a Wigner crystal of nuclei immersed in the homogeneous electron background [12]. It is clear that such Coulomb effects do not disappear with increasing density and temperature, and it is a-priori not evident that a

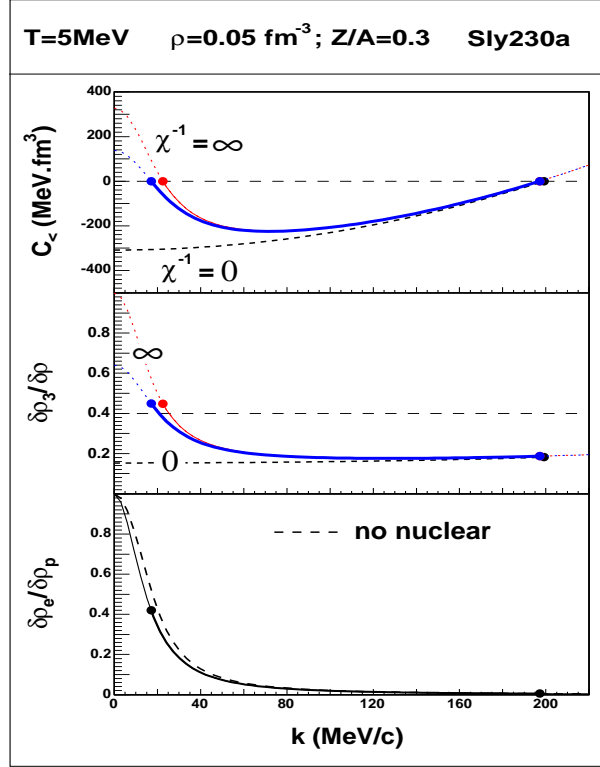


Figure 1. Eigen-mode of the minimal free-energy curvature for $\rho = 0.05 \text{ fm}^{-3}$, $Z/A = 0.3$, $T = 5 \text{ MeV}$, as a function of the wave number k , calculated with the Sly230a Skyrme interaction. Top: eigen-value. Middle: associated eigen-vector in the nuclear-density plane. The curves are compared to two limiting cases corresponding to a zero and infinite incompressibility of the negatively charged gas. When the curvature is negative (full lines) this eigen-vector gives the phase-separation direction. The dots give the points of zero curvature. The dashed line gives the direction of constant Z/A . Bottom: same as the middle part, in the plane of proton and electron density. The dashed line gives the eigenvector when the nuclear force is zero. Figure taken from ref. [18].

phenomenology equivalent to the one calculated for uncharged nuclear matter might at all be observed. However, guided by the uncharged nuclear matter example, the standard treatments currently used in most supernovae codes describe the dilute stellar matter at finite temperature in the baryonic sector as a statistical equilibrium between protons, neutrons, alphas and a single heavy nucleus representing the finite system counterpart of the liquid fraction [13, 14]. The transition to homogeneous matter in the neutron star core is supposed to be first-order in these modelizations and obtained through a Maxwell construction in the total density at fixed proton fraction.

From the nuclear physics side it is well recognized that, since stellar matter is subject to the contrasting couplings of the electromagnetic and the strong interaction acting on comparable length scales because of the electron screening, this should give rise to the phenomenon of frustration [15], well-known in condensed matter physics [16]. Because of this, a specific phase diagram, different from the one of nuclear matter and including in-homogeneous components, is expected in stellar matter [17].

2.1. Coulomb effects in dilute stellar matter

The quenching of the first-order phase transition due to Coulomb effects is illustrated in Figure 1 in a finite temperature Hartree-Fock calculation with realistic phenomenological interactions [18]. In order to determine the possible first-order phase transition in stellar matter, the instability of such matter with respect to a density fluctuation can be studied by considering the free energy variation once independent proton, neutron, and electron fluctuations (q, p, e)

$$\delta\rho_q = A_q e^{i\vec{k}\cdot\vec{r}} + c.c., \quad (1)$$

are imposed in a given thermodynamic condition defined by a density, temperature, and proton fraction. This variation in the three-dimensional space of density fluctuations $\tilde{A} = (A_n, A_p, A_e)$ reads [19] :

$$\delta f = \tilde{A}^* \mathcal{C}^f \tilde{A}, \quad (2)$$

where

$$\mathcal{C}^f = \begin{pmatrix} \partial\mu_n/\partial\rho_n & \partial\mu_n/\partial\rho_p & 0 \\ \partial\mu_p/\partial\rho_n & \partial\mu_p/\partial\rho_p & 0 \\ 0 & 0 & \partial\mu_e/\partial\rho_e \end{pmatrix} + k^2 \begin{pmatrix} 2C_{nn}^f & 2C_{np}^f & 0 \\ 2C_{pn}^f & 2C_{pp}^f & 0 \\ 0 & 0 & 0 \end{pmatrix} + \frac{4\pi^2 e^2}{k^2} \begin{pmatrix} 0 & 0 & 0 \\ 0 & 1 & -1 \\ 0 & -1 & 1 \end{pmatrix} \quad (3)$$

is the free-energy curvature matrix. An instability against matter clusterization corresponds to a negative free-energy curvature in the space of density fluctuations. It is studied through the k -dependent curvature matrix \mathcal{C}^f . A negative eigenvalue associated to a given wavelength signals that a fluctuation characterized by the associated eigenvector will be spontaneously amplified, giving rise to cluster formation if the wavelength is finite, or phase separation for infinite wavelengths. This smallest eigenvalue $C_<$ is shown as a function of the wave number in Figure 1. We can see that the eigenvalue is positive at $k=0$, meaning that the phase transition is quenched and replaced by cluster formation in stellar matter.

This Coulomb frustration effect has been confirmed by different microscopic models [20]. A continuous evolution from the Coulomb lattice to a homogeneous nuclear fluid, passing through the formation of clusters of different sizes and strongly deformed dis-homogeneous structures close to the saturation density has been reported, both at zero and at finite temperature.

These calculations are numerically very heavy and a complete thermodynamic characterization of stellar matter under the frustrated phase transition has not been done yet. Such a task can however be performed in the phenomenological so-called nuclear statistical equilibrium (NSE) approaches, which treat the bound states of nucleons as new species of quasi-particles [21, 22, 23, 24].

2.2. Application in the extended NSE model

Within NSE, the baryonic component of the stellar matter is regarded as a statistical equilibrium of neutrons and protons, the electric charge of the latter being screened by a homogeneous electron background. As a first approximation, one can consider that the system of interacting nucleons is equivalent to a system of non-interacting clusters, with the nuclear interaction being completely exhausted by clusterization. This simple model can describe only diluted matter at $\rho \ll \rho_0$ as it can be found in the outer crust of neutron stars, while nuclear interaction among nucleons and clusters has to be included for applications at higher density, when the average inter-particle distance becomes comparable to the range of the force. A simple possibility [25, 26] is to take into account interactions among composite clusters in the simplified form of a hard-sphere excluded volume, and interactions among nucleons in the self-consistent Hartree-Fock approximation with a phenomenological realistic energy functional fitted on a large number of measured mass and radii. In this version of the model, the thermodynamics can be calculated

in the ensemble (β, μ_I, ρ) defined by inverse temperature $\beta = T^{-1}$, isovector chemical potential $\mu_I = \mu_n - \mu_p$ and baryonic density $\rho = \rho_n + \rho_p$. The total entropy density is given by

$$\sigma_{\beta, \mu_I}^{can}(\rho) = \ln \mathcal{Z}_{\beta, \mu_I}^{a=1}(\rho_f) + \lim_{V \rightarrow \infty} \frac{1}{V} \ln \mathcal{Z}_{\beta, \mu_I}^{a>1}(V \rho_{cl}) \quad (4)$$

where the density repartition between the clustered ρ_{cl} and unbound ρ_f component $\rho = \rho_{cl} + \rho_f$ is uniquely defined by the condition of having a single chemical potential μ for both components. The unbound nucleons partition sum is calculated in the mean-field approximation:

$$\ln \mathcal{Z}_{\beta, \mu_I}^{a=1}(\rho) = \ln \mathcal{Z}_{\beta, \mu, \mu_I}^0 - \beta \left(\frac{\partial}{\partial \beta} \ln \mathcal{Z}_{\beta, \mu, \mu_I}^0 + V \epsilon^{HF} \right) - \beta \mu \rho V, \quad (5)$$

In this equation ϵ^{HF} is the Hartree-Fock energy and the non-interacting part of the partition sum can be expressed as a functional of the kinetic energy density τ_q for neutrons (q) or protons ($q = p$) :

$$\ln \mathcal{Z}_{\beta, \mu, \mu_I}^0 = \frac{2\beta V}{3} \sum_{q,p} \tau_q \frac{\partial \epsilon^{HF}}{\partial \tau_q}, \quad (6)$$

where τ_q are self-consistently derived as a function of the associate chemical potential μ_q and effective mass m_q^* .

The partition sum of clusters for a total particle number $A = V \rho_{cl}$ is calculated via a recursive relation:

$$\mathcal{Z}_{\beta, \mu_I}(A) = \frac{1}{A} \sum_{a=2}^A a \omega_a \mathcal{Z}_{\beta, \mu_I}(A - a). \quad (7)$$

where the weight of the different cluster size is given by:

$$\omega_a = V_F \sum_{i=-a}^a \left(\frac{2\pi a m_0}{\beta \hbar^2} \right)^{3/2} \exp \left(-\beta f_{a,i}^\beta \right) \exp(\beta i \mu_I). \quad (8)$$

Here, $f_{a,i}^\beta$ is a phenomenological free energy functional including the screening effect of electrons in the Wigner-Seitz approximation, and $V_F = V(1 - \rho_{cl}/\rho_0)$ is the volume fraction available to the clusters [25, 26] .

The thermodynamics of the extended NSE model is presented in Figure 2. We can see that the equation of state does not present any plateau as it would have been the case for a first-order phase transition. More surprising, the entropy presents a convex intruder, the behavior of the equation of state is not monotonic and a clear back-bending is observed, qualitatively similar to the phenomenon observed in phase transitions in finite systems [27]. It is interesting to remark that similar behaviors, with non-monotonic equations of state and discontinuities in the intensive variables, are systematically observed in phase transitions with long-range interactions [16]. A consequence of the back-bending in the equation of state is that this unusual thermodynamics can only be observed in the canonical ensemble where the density is controlled. Indeed if the baryon chemical potential was controlled as it is the case in standard NSE, in the region of the back-bending the multiple evaluation of the chemical potential would lead to keep only the solution of minimal free energy. This means that the whole back-bending region would be jumped over and one would observe a density discontinuity, that is a first-order phase transition. This in-equivalence of statistical ensembles is a characteristic feature of phase transitions with long range interactions. Different model applications have indeed shown fingerprints of ensemble in-equivalence [16], but phenomenological applications are scarce. The NSE calculation of Figure

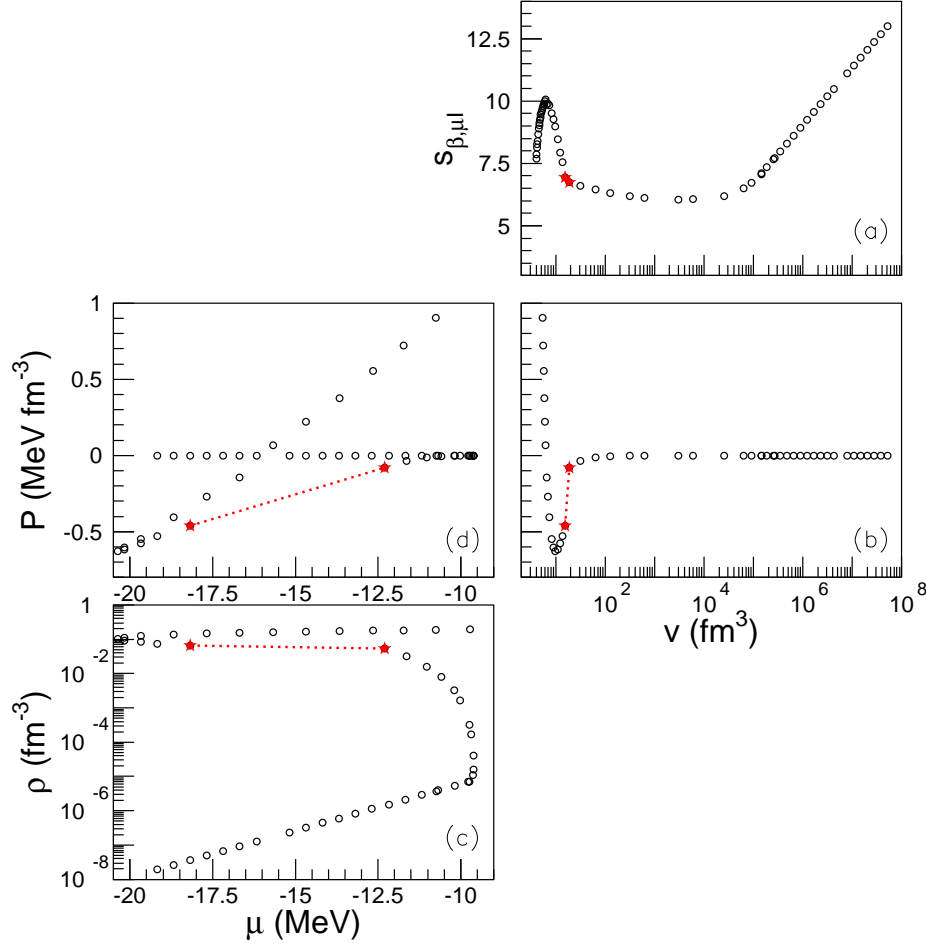


Figure 2. Constrained entropy (a), pressure [(b) and (d)] and chemical potential [(c) and (d)] evaluated in the extended NSE model in the canonical ensemble at $T = 1.6$ MeV and asymmetry chemical potential $\mu_I = 1.68$ MeV. Stars and dotted line signal pressure and chemical potential discontinuity. Figure taken from ref. [26].

2 shows that the inhomogeneous baryonic matter which is produced in the explosion of core-collapse supernova and in neutron stars is an example of a physical system which displays this in-equivalence.

From the physical viewpoint, the correct modelization is the canonical one. Indeed if the grandcanonical phase coexistence solution was the preferred response at equilibrium inside the in-equivalence region, such solution would have been found in a canonical calculation where the coexistence density is imposed. On the contrary, once the density is fixed, a dis-homogeneous clusterized solution is found in agreement with the expected phenomenology associated to the Coulomb frustration. This is demonstrated in the left part of Figure 3, which shows the cluster distribution in the in-equivalence region. As a function of the density, the average cluster size is continuously changing and can never be assimilated to a portion of the fluid phase. The right part of the same figure compares the grandcanonical and canonical cluster distribution in a thermodynamic situation relevant for supernova physics. We can see that accounting for the correct thermodynamics has important consequences on the matter composition. Since the cluster abundances determine the electron capture rate, which in turn is a capital ingredient

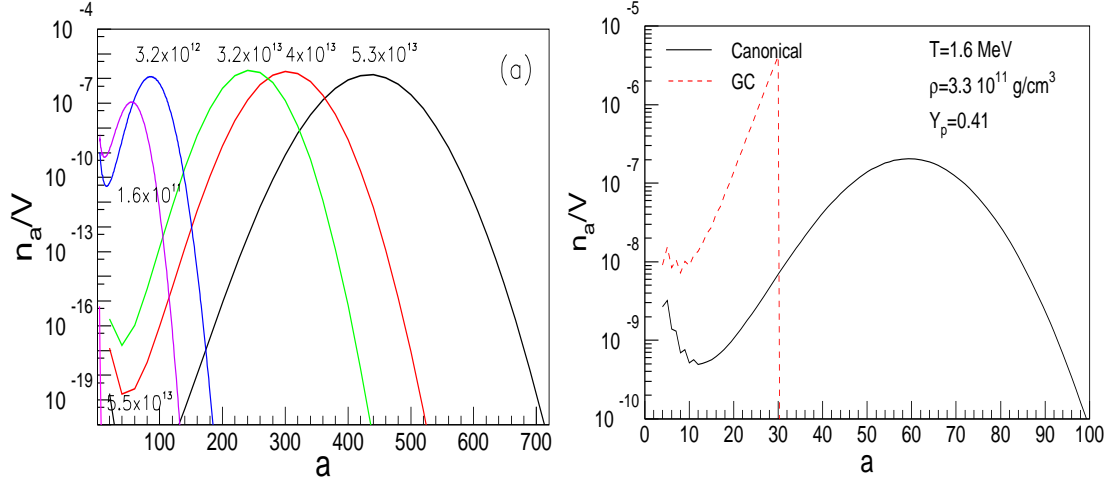


Figure 3. Left side: Cluster distributions as a function of the density (expressed in g/cm^3) of the extended NSE model in the ensemble in-equivalence region in the same thermodynamic conditions than in Figure 2. Right side: Comparison between canonical (full line) and grand-canonical (dashed line) predictions for the cluster distribution in a specific thermodynamic condition relevant for supernova dynamics. Figure taken from ref. [26].

for the size of the homologous core and the cooling process, it is clear that a control of the phase diagram is important for supernova physics. It is also interesting to remark that the most probable abundances concern not so neutron-rich nuclei which are potentially accessible in laboratory experiments: a detailed knowledge of the mass, level density and electron capture cross section for these nuclei is thus needed to have a reliable description of the equation of state.

2.3. In-medium effects

In the extended NSE model presented in the previous section clusters are treated as an ideal gas characterized by an empirical energy functional which is modified with respect to nuclei in the vacuum only through the excluded volume mechanism. This is an improvement compared to standard NSE [21, 22, 23, 24] in which the Coulomb screening by the electron background is the only interaction accounted for, but still represents a crude approximation of the effect of the medium [28]. Microscopic modifications of the cluster binding energies due to Pauli blocking shifts have been computed [9] and shown to correctly describe the Mott dissolution of deuterons in dense matter, but this heavy numerical approach cannot be extended to massive clusters. In the original Lattimer-Swesty model [13] the assumption is made that the effect of the medium consists in a modification of the cluster surface tension, the bulk energy being unaffected. However some interpretations of multifragmentation data suggest that bulk terms might also be affected [29].

To microscopically account for in-medium modifications of the cluster binding energies, we have realized a systematic set of Hartree Fock calculations in the Wigner Seitz cell for various isotopic chains with a total neutron number ranging from the stability line up to $N \approx 3000$. The resulting microscopic nuclear energy, consisting of a volume and a surface term, is parameterized with an in-medium modified mass formula

$$E_{HF} = \epsilon^{HF}(\rho_n, \rho_p)(V_{WS} - V_{cl}) - [a_V^m(\rho) - a_{Vsym}^m(\rho, \delta)\delta_0^2] A + [a_S^m(\rho) - a_{Ssym}^m(\rho, \delta)\delta_0^2] A^{2/3} \quad (9)$$

where V_{WS} is the volume of the calculation cell and $\rho_n, \rho_p, \rho, \delta$ is the neutron, proton, total

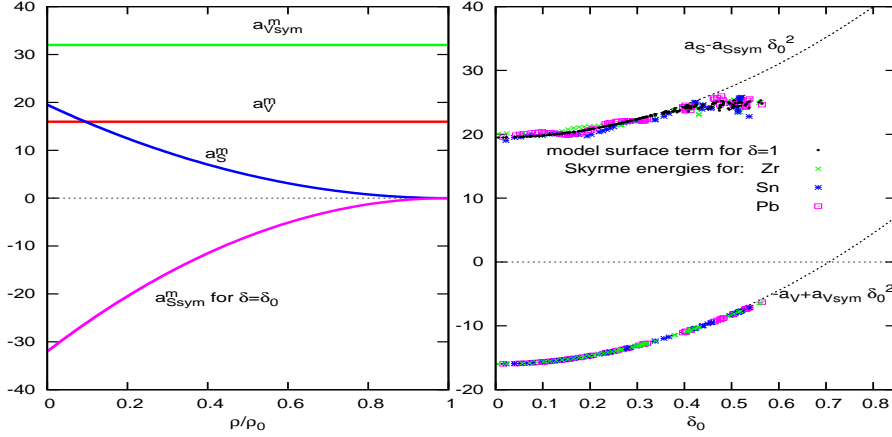


Figure 4. Left part: isoscalar and isovector bulk and isoscalar surface term of the in-medium modified mass formula extracted from Hartree-Fock calculations in the Wigner-Seitz cell. Right part: comparison between the microscopic Hartree-Fock volume energy per particle and surface energy per $A^{2/3}$ and the parameterization eq.(9) for three isotopic chains as a function of the bulk proton-neutron asymmetry. The model surface term is given by $[a_S^m(\rho) - a_{Ssym}^m(\rho, \delta)\delta_0^2]$, see eq. (9).

density and asymmetry $\delta = (\rho_n - \rho_p)/\rho$ of the free nucleons constituting the dripping gas. The cluster mass and charge A, Z and the gas densities are extracted through a Wood-Saxon fit of the local density. The bulk density ρ_0 and asymmetry $\delta_0 = (\rho_{0n} - \rho_{0p})/\rho_0$ in the model are approximated by analytical functions of A, Z , while $V_{cl} = A/\rho_0$. The resulting in-medium parameters obtained from a preliminary fit of the microscopic Hartree-Fock results through eq.(9) are shown in the left part of Figure 4, while the quality of the fit is displayed in the right part of the same figure.

To obtain the fit shown in Fig.4 we have employed the ansatz

$$a_S^m(\rho) = a_S \left(1 - \frac{\rho}{\rho_0}\right)^{\gamma_1} ; \quad a_{Ssym}^m(\rho, \delta) = a_{Ssym} \left(1 - \frac{\rho\delta}{\rho_0\delta_0}\right)^{\gamma_2} \quad (10)$$

with $\gamma_1 = \gamma_2 = 2$ and with $a_{Ssym} = -32$ MeV. A dependence of a_{Ssym}^m on ρ_0, δ_0 is implicit. We can see that the in-medium modified liquid drop expression eq.(9) provides a reasonably accurate description of the energy modification due to the external gas. In agreement with the conjecture of ref. [13], the bulk terms are completely unaffected by the external medium ($a_V^m(\rho) = a_V = \text{cst.}$, $a_{Vsym}^m(\rho, \delta) = a_{Vsym} = \text{cst.}$), while important effects on the surface properties of nuclei are seen. The implementation of such an improved energy functional in the extended NSE model is in progress.

3. Supra-saturation densities and the strangeness phase transition

If it is well admitted that hyperonic and deconfined quark matter could exist in the inner core of neutron stars, a complete understanding of the composition and equation of state of dense matter is far from being achieved. Concerning hyperons, simple energetic considerations suggest that they should be present at high density [30]. However, in the standard picture the opening of hyperon degrees of freedom leads to a considerable softening of the equation of state [30, 31, 32, 33, 34, 35], which in turns leads to maximum neutron star masses smaller than the observed masses of many neutron stars, in particular the high values

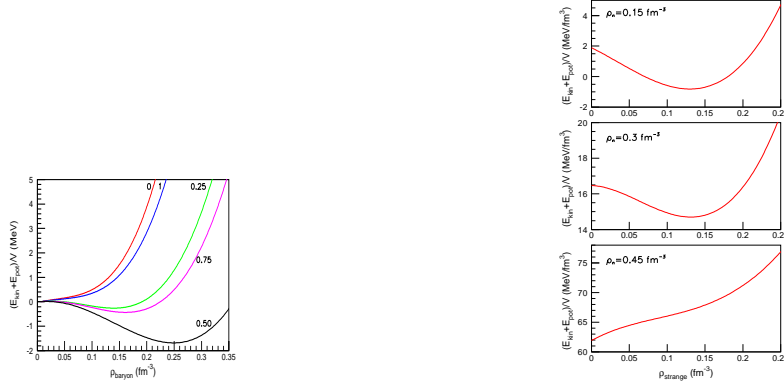


Figure 5. Left part: energy density as a function of the total baryon density for a (n, Λ) mixture at $T = 0$ with different Λ fractions with the energy functional proposed in ref. [42]. Right part: same as a function of the strange density at fixed neutron densities.

obtained in recent observations [1]. This puzzling situation implies that the hyperon-hyperon and hyperon-nucleon couplings must be much more repulsive at high density than presently assumed [36, 37, 38, 39, 40, 41], and/or that something is missing in the present modelization.

The generic presence of attractive and repulsive couplings suggests the existence, in a model-independent manner, of a phase transition involving strangeness. Let us consider a simplified situation where matter is uniquely composed of neutrons and Λ -hyperons. The energy density $\epsilon = \epsilon_{kin} + \epsilon_{pot}$ at zero temperature obtained with the energy density functional proposed by Balberg and Gal [42]

$$\begin{aligned} \epsilon_{pot}(\rho_n, \rho_\Lambda) &= \frac{1}{2} \left[(a_{NN} + b_{NN}) \rho_n^2 + c_{NN} \rho_n^{\delta+1} \right] + \frac{1}{2} \left[a_{\Lambda\Lambda} \rho_\Lambda^2 + c_{\Lambda\Lambda} \rho_\Lambda^{\gamma+1} \right] \\ &+ a_{\Lambda n} \rho_n \rho_\Lambda + c_{\Lambda n} \frac{\rho_n \rho_\Lambda}{\rho_n + \rho_\Lambda} [\rho_n^\gamma + \rho_\Lambda^\gamma], \end{aligned} \quad (11)$$

for different hyperon fractions $Y_\Lambda = \rho_\Lambda / (\rho_\Lambda + \rho_n)$ is represented in the left part of Fig. 5. For all numerical applications, the parameter values from parameterization BG I, see ref. [44] are used. We can see that, due to the attractive part of the $n\Lambda$ coupling, a mixture of the two

particle species admits a bound state at finite density. This rather general feature of the energy density is found within other parameterizations and other models, e.g. the parameterization of the energy density functional from G-matrix calculations by Vidana et al. [43]. The existence of a minimum in the energy functional for symmetric matter means that such a state represents the stable matter phase at zero temperature. On the other side, the vanishing density gas phase is always the stable phase in the limit of infinite temperature. This implies that a dilute-to-dense phase change in strange matter has to be expected on very general grounds. The right part of Fig.5 shows that the minimum, for a certain interval of neutron densities, is also observed as a function of the Λ density. This is again due to the interplay between the attractive $\Lambda - \Lambda$ interaction required by hypernuclear data, and the repulsion at high density required by the two-solar mass neutron star observation. This information means that the expected phase change is expected to have strangeness contributing to the order parameter.

The presence of a minimum is however not sufficient to discriminate between a smooth cross-over and a phase transition. In the next section we will therefore demonstrate the existence of a phase transition by explicitly calculating the $n\Lambda$ phase diagram.

3.1. Neutron- Λ phase diagram

First-order transitions are signaled by an instability or concavity anomaly in the mean-field thermodynamic potential, which has to be cured by means of the Gibbs phase equilibrium construction at the thermodynamic limit. At zero temperature, one thermodynamic potential is given by the total energy

$$\epsilon_{tot}(\rho_n, \rho_\Lambda) = \epsilon_{pot}(\rho_n, \rho_\Lambda) + \epsilon_{kin}(\rho_n, \rho_\Lambda) + (\rho_n m_n + \rho_\Lambda m_\Lambda) c^2 \quad (12)$$

The spinodal region is then recognized as the locus of negative curvature of the energy surface, $C_{min} < 0$. The corresponding eigenvector defines a direction in the density space given by

$$\frac{\rho_n}{\rho_\Lambda} = \frac{C_{n\Lambda}}{C_{min} - C_{nn}} = \frac{C_{min} - C_{\Lambda\Lambda}}{C_{\Lambda n}} \quad (13)$$

with $C_{ij} = \partial^2 \epsilon_{tot} / \partial \rho_i \partial \rho_j$. This instability direction physically represents the chemical composition of density fluctuations which are spontaneously and exponentially amplified in the unstable region in order to achieve phase separation, and gives the order parameter of the associated phase transition.

The zero temperature instability region of the $n\Lambda$ mixture is shown in the left part of Fig. 6. We can see that a large portion of the phase diagram is concerned by the instability. We can qualitatively distinguish three regions characterized by different order parameters. Below nuclear saturation density, we observe an isoscalar $\rho_n \approx \rho_\Lambda$ instability, very close to ordinary nuclear liquid-gas, with Λ 's playing the role of protons. Increasing neutron density the phase separation progressively changes towards the strangeness $\rho_S = -\rho_\Lambda$ direction: the two stable phases connected by the instability have close baryon densities but a very different fraction of Λ 's. For high ρ_Λ we observe the same behavior with the roles of neutrons and Λ -hyperons exchanged. The part of the phase diagram at high neutron density comprises the region physically explored by supernova and neutron star matter, which is characterized by chemical equilibrium for reactions implying strangeness, $\mu_S = \mu_n - \mu_\Lambda = 0$. The strangeness equilibrium trajectory is represented by a dashed line in Fig.6. This physically corresponds to the sudden opening of strangeness, observed in many modelizations of neutron star matter (see e.g. [42, 35]).

Let us stress that the existence of a strangeness phase transition at high density is not a general model-independent feature, although many models show it. There are others, for instance the G-matrix models of ref. [43], which do not show an instability in this region. The reason is essentially due to the absence of a $\Lambda\Lambda$ interaction in these microscopic calculations. Owing to

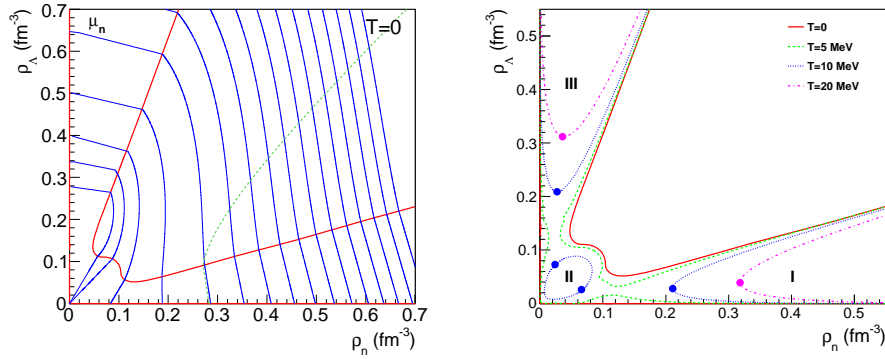


Figure 6. Left part: (n, Λ) mixture at $T = 0$: Borders of the phase coexistence region (red thick lines), constant- μ_n paths after Maxwell construction (blue thin lines) and $\mu_n = \mu_\Lambda$ trajectory after Gibbs construction (dark green dotted line). Right part: borders of the phase coexistence region of the $n\Lambda$ mixture for different temperatures, $T=0, 5, 10, 20$ MeV. The full circles mark the critical points. Figures taken from ref. [44].

the lack of reliable information on the hyperonic interactions, which would discriminate between different models, we cannot affirm the existence of the strangeness phase transition, related to this instability, but, turning the argument around, the presence of this phase transition in a physical system would allow to learn much about the shape of the interaction.

Up to now we have only presented results at zero temperature. The extension to finite temperature, as it is needed for supernova matter, is relatively simple in the mean-field approximation. The appropriate thermodynamic potential at non-zero temperature is given by the Helmholtz free energy

$$f_T(\rho_n, \rho_\Lambda) = \epsilon_{tot}(\rho_n, \rho_\Lambda) - Ts(\rho_n, \rho_\Lambda) \quad (14)$$

where s is the mean-field entropy density. Chemical potentials can be obtained by differentiating this expression. Then the Gibbs construction is performed from the combined analysis of $\mu_n(\rho_n)$ at constant μ_Λ , and $\mu_\Lambda(\rho_\Lambda)$ at constant μ_n .

The phase diagram as a function of temperature is presented in the right panel of Fig. 6. This phase diagram exhibits different interesting features. We can see that the three regions that we have tentatively defined at zero temperature appear as distinct phase transitions at finite temperature. The first phase transition (zone II in Fig.6 - right panel) separates a low density gas phase from a high density more symmetric liquid phase, very similar to ordinary liquid-gas. The second one (zone III in Fig.6 - right panel) reflects the instability of dense strange matter towards the appearance of neutrons and has an almost symmetric counterpart (zone I in Fig.6 - right panel) in the instability of dense neutron matter towards the formation of Λ -hyperons. Up to a certain temperature, this latter phase transition is explored by the $\mu_n = \mu_\Lambda$ trajectory,

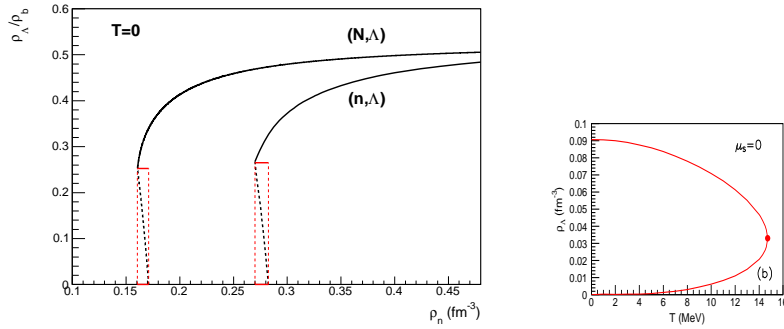


Figure 7. Left: Λ fraction as a function of the baryon density within the condition $\mu_n = \mu_\Lambda$ for a $n\Lambda$ and, respectively, a symmetric $\rho_n = \rho_p$ $np\Lambda$ mixture at $T=0$. The full lines correspond to the stable mean-field results; the dashed lines illustrate the Gibbs constructions; the horizontal lines indicate the relative amount of Λ -hyperons at the frontiers of the phase-coexistence domain. Right: Λ density for the two coexisting phases as a function of temperature for $\mu_S = 0$. Figures taken from ref. [44].

meaning that it is expected to occur in neutron stars and supernova matter. At variance with other known phase transitions in nuclear matter, this transition exists at any temperature and is not limited in density; it is always associated with a critical point, which moves towards high density as the temperature increases. This means that criticality should be observed in hot supernova matter, at a temperature which is estimated as $T_c = 14.8$ MeV in the present schematic model.

The consequences of these findings for the composition of neutron star matter are drawn in Fig. 7. The left panel shows the Λ fraction $Y_\Lambda = \rho_\Lambda / (\rho_n + \rho_\Lambda)$ as a function of the baryon density under the condition $\mu_n = \mu_\Lambda$. The crossing of the mixed-phase region with increasing neutron density implies that, as soon as the lower density transition border is crossed, the system has to be viewed as a dis-homogeneous mixture of macroscopic regions composed essentially of neutrons, with other macroscopic regions with around 25% of hyperons. The extension of the Λ -rich zone increases with density until the system exits the coexistence zone, and becomes

homogeneous again. The density values associated to the phase transition slightly change with the energy functional assumed. To give a simple example, we present on the same Fig.7 a calculation where Λ 's are put in equilibrium with symmetric $\rho_n = \rho_p$ non-strange matter, that is eq.(11) is still used, but the symmetry energy in the nucleon sector b_{NN} is put to zero [42]. We can see that only small differences are observed in the strange phase transition considering pure neutron matter or symmetric matter.

On the right panel of Fig. 7 the Λ -densities for the two coexisting phases are displayed as a function of temperature, again under the condition of $\mu_n = \mu_\Lambda$, physically relevant for neutron star and supernova matter. The extension of the coexistence region decreases with increasing temperature. The latter finally disappears at $T_c = 14.8$ MeV. This well illustrates the fact that the critical point of the strangeness phase transition moves to higher density, crossing the physical line $\mu_n = \mu_\Lambda$ at a given temperature.

4. Conclusions

In this contribution we have analyzed the phase diagram of stellar matter as it is produced in core-collapse supernovae and proto-neutron stars in the thermodynamical conditions where such matter can be described by nucleonic and hadronic degrees of freedom.

At baryonic densities lower than nuclear saturation, we have shown on very general arguments that the first-order phase transition of neutral nuclear matter is quenched in stellar matter due to the effect of Coulomb frustration. As a consequence, matter is expected to be clusterized even at finite temperature in the whole sub-saturation regime.

The composition and thermodynamics of such clusterized matter has been explicitly worked out in the framework of a quasi-particle model where inter-particle interactions are modeled through excluded volume. Coulomb correlations with the neutralizing electron gas are accounted for in the Wigner-Seitz approximation and residual nuclear correlations are included in an effective way through an in-medium modification of the cluster energy functional with parameters fitted from Hartree-Fock calculations with a realistic effective interaction. The same formalism is used to evaluate the free nucleon self-energies.

The expectation of the phase transition quenching is confirmed by this model, which shows that the single nucleus approximation widely used is a poor approximation at finite temperature and a large distribution of cluster species has to be included in supernova modeling. In addition to that, the Coulomb frustration effect is seen to drastically modify the functional relation between pressure, chemical potential and density with respect with a first-order phase transition. Specifically, backbendings are observed in the equations of state which cannot be correctly evaluated in the grandcanonical ensemble but require a canonical evaluation of the partition sum.

In the supersaturation regime, we have used the same mean field approximation with effective phenomenological energy functionals in order to describe the characteristics of the phase diagram in the presence of strangeness.

We have shown that already a simple system composed of neutrons and Λ hyperons in thermal equilibrium presents a complex phase diagram with first and second order phase transitions. Some of these phase transitions are probably never explored in physical systems. However, a possible phase transition at super-saturation baryon densities, from non-strange to strange matter is expected to be observed both in the inner core of neutron star and in the dense regions of core-collapse supernova. For this latter phenomenology, a critical point is predicted and the associated critical opalescence could have an impact on supernova dynamics [5]. The immediate consequence of that is that the opening of hyperon channels at high density should not be viewed as a continuous (though abrupt) increase of strangeness in the matter, observed in many models of hyperonic matter, cf e.g. [35], but rather as the coexistence of hyperon-poor and hyperon-rich macroscopic domains.

An extension of this simple model to include all possible hyperons and resonances is in progress.

References

- [1] Demorest P et al 2010 *Nature* **467** 1081; Ozel F et al 2010 *Astrophys. J.* **724** L 199.
- [2] Page D et al 2011 *Phys. Rev. Lett.* 106 081101; P.S.Shternin et al 2011 *Monthly Notices of the RAS: Letters* **412** L108 .
- [3] Nakazato K et al 2012 *Astrophys. J.* **745** 197.
- [4] Marek A and Janka H Th 2009 *Astrophys. Journ.* **694** 664.
- [5] Margueron J, Navarro J, and Blottiau P 2004 *Phys. Rev. C* **70** 028801.
- [6] Siemens P J 1983 *Nature* **305** 410.
- [7] Ducoin C, Chomaz P, Gulminelli F 2006 *Nucl. Phys. A* **771** 68.
- [8] Rios A 2010 *Nucl. Phys. A* **845** 58.
- [9] Typel S et al 2010 *Phys. Rev. C* **81** 015803.
- [10] Bonnet E et al 2009 *Phys. Rev. Lett.* **103** 072701.
- [11] Maruyama T et al 2005 *Phys. Rev. C* **72** 015802.
- [12] Lattimer J M and Prakash M 2004 *Science* Vol. **304** no. 5670 536.
- [13] Lattimer J M and Swesty F D 1991 *Nucl. Phys. A* **535** 331.
- [14] Shen H, Toki H, Oyamatsu K and Sumiyoshi K 1998 *Prog. Theor. Phys.* **100** 1013.
- [15] Horowitz C J et al 2006 *Phys. Rev. C* **72** 035801.
- [16] Campa A et al 2009 *Phys.Rep.* **480** 57.
- [17] Napolitani P et al 2007 *Phys. Rev. Lett.* **98** 131102; Ducoin C et al 2007 *Phys. Rev. C* **75** 065805.
- [18] Ducoin C, Chomaz P and Gulminelli F, *Nucl. Phys. A* **789** 403; Ducoin C et al 2008 *Phys. Rev. C* **78** 055801.
- [19] Pethick C J, Ravenhall D G and Lorentz C P 1995 *Nucl. Phys. A* **584** 675.
- [20] Watanabe G 2010 *Prog. Theor. Phys. Suppl.* **186** 45.
- [21] Phillips A C 1994 *The Physics of Stars* (Chichester: John Wiley & Sons).
- [22] Botvina A S and Mishustin I N 2010 *Nucl. Phys. A* **843** 98.
- [23] Blinnikov S I, Panov I V, Rudzsky M A and Sumiyoshi K 2011 *Astron. Astrophys.* **535** A37.
- [24] Souza S R, Steiner A W, Lynch W G, Donangelo R and Famiano M A 2009 *Astrophys. J.* **707** 1495.
- [25] Raduta A R and Gulminelli F 2010 *Phys. Rev. C* **82** 065801.
- [26] Gulminelli F and Raduta A R 2012 *Phys. Rev. C* **85** 025803.
- [27] Chomaz P, Duflot V and Gulminelli F 2000 *Phys. Rev. Lett.* **85** 3587; Gross D H E 2001 *Lecture Notes in Physics* Vol. **66** 1; Raduta A H and Raduta A R 2002 *Nucl. Phys. A* **703** 876.
- [28] Hempel M and Schaffner-Bielich J 2010 *Nucl. Phys. A* **837** 210.
- [29] Shetty D V et al *Preprint* nucl-ex/0406008.
- [30] Glendenning N 1982 *Phys.Lett. B* **114** 392.
- [31] Baldo M, Burgio G F and Schulze H J 2000 *Phys. Rev. C* **61** 055801.
- [32] Vidana I, Polls A, Ramos A, Engvik L and Hjorth-Jensen M 2000 *Phys. Rev. C* **62** 035801.
- [33] Djapo H, Schaefer B J and Wambach J 2010 *Phys. Rev. C* **81** 035803.
- [34] Schulze H J and Rijken T 2011 *Phys. Rev. C* **84** 035801.
- [35] Massot E, Margueron J and Chanfray G 2012 *Europhys. Lett.* **97** 39002.
- [36] Hofmann F, Keil C and Lenske H 2001 *Phys. Rev. C* **64** 025804.
- [37] Bonanno L and Sedrakian A 2012 *Astron. Astrophys.* **539** A16.
- [38] Weissenborn S, Chatterjee D and Schaffner-Bielich J 2012 *Nucl. Phys. A* **881** 62; 2012 *Phys. Rev. C* **85** 065802.
- [39] Bednarek I, Haensel P, Zdunik J L, Bejger M and Manka R *Preprint* astro-ph/1111.6942.
- [40] Lastowiecki R, Blaschke D, Grigorian H and Typel S 2012 *Acta Phys. Polon. Supp.* **5** 535.
- [41] Oertel M, Fantina A and Novak J 2012 *Phys. Rev. C* **85** 055806.
- [42] Balberg S and Gal A 1997 *Nucl. Phys. A* **625** 435.
- [43] Vidana I, Logoteta D, Providencia C, Polls A and Bombaci I *Preprint* astro-ph/1004.3958.
- [44] Gulminelli F, Raduta A R and Oertel M 2012 *Preprint* arXiv:1206.4924.